Confinement of acoustical vibrations in a semiconductor planar phonon cavity

M. Trigo[1], A. Bruchhausen[1], A. Fainstein[1], B. Jusserand[2], and V. Thierry-Mieg[2]
[1] *Centro Atómico Bariloche & Instituto Balseiro, C.N.E.A., 8400 S. C. de Bariloche, R. N., Argentina*
[2] *Laboratoire de Photonique et de Nanostructures, CNRS, Route de Nozay, 91460 Marcoussis, France*

Extending the idea of optical microcavities to sound waves, we propose a *phonon cavity* consisting of two semiconductor superlattices enclosing a spacer with thickness determined by the acoustic wavelength at the center of the first zone-center folded minigap. We show that acoustical phonons can be confined in these layered structures, and propose Raman experiments which are able to probe these novel excitations. The Raman experiments take profit of an optical microcavity scattering geometry that, through the forward-scattering contribution, gives access to the zone-center excitations. We report experimental results of Raman scattering in a structure based in GaAs/AlAs materials that demonstrate unambiguously the observation of phonon cavity confined acoustical vibrations. The experimental results compare precisely with photoelastic model calculations of the Raman spectra of the proposed phonon-cavity embedded optical microcavity.

78.30.Fs,63.20.Dj,78.66.Fd,42.60.Da

The wave character of electrons and their interaction with a periodic potential in crystals leads to the Bragg reflection and opening of forbidden energy gaps. [1] An impurity state with energy within this gap is reflected back in all three propagation directions and thus its wavefunction is confined in space. The equivalent of a periodic potential for optical waves (i.e., photons) is a periodic structure of materials with contrasting refractive index. A planar periodic stack of two materials $\lambda/4$ thick reflects photons propagating normal to the layers within a stop-band around the wavelength λ, and is termed a "distributed Bragg reflector" (DBR). [2] Photon gaps can also be opened in the three space directions by appropriately selecting the dielectric material and structure. [3] A planar microcavity is a spacer of thickness $\lambda/2$ enclosed by two DBR's. [4] Photons of wavelength λ are confined in such structure much like an electronic defect state in a crystal. [5] This photon confinement leads to fundamental changes in the light-matter interaction. [4] Phonons are vibrational waves described by similar wave equations as photons, but which are subject to mechanical (instead of electromagnetic) boundary conditions at the interfaces. Extending the above ideas to vibrational waves, in this letter we propose a planar "phonon cavity" structure designed to confine acoustical phonons. In addition, we show theoretically that Raman scattering through an optical cavity geometry [6,7] is able to probe these novel excitations, and we demonstrate their existence through experiments in a real GaAs/AlAs based structure. These results are relevant to diverse phenomena as, e.g., phonon amplification and stimulated emission [8–10], coherent generation and control of phonons [11], and modified electron-phonon interactions.

The acoustical phonon branches in a superlattice (SL) made of a periodic sequence of semiconductor layers can be described by backfolding the phonon dispersion of an average bulk solid and opening of small minigaps at the zone-center and reduced new Brillouin-zone edge. [12] It has been proposed long time ago that the minigap of these zone-folded SL acoustical phonons can be used as a "phonon filter", acting very much like dielectric DBR's but for the selective reflection of high frequency sound waves. [13] Thus, a planar "phonon cavity" can be constructed by enclosing between two SL's a spacer of thickness $\lambda_{ac}/2$, where now λ_{ac} is the wavelength of the acoustical phonon at the center of the phonon minigap. In Fig.1 we present a scheme of the proposed phonon cavity structure, based in semiconductor GaAs and AlAs materials. The "phonon DBR's" consist of 11 period $74\AA/38\AA$ GaAs/AlAs SL's, and enclose a $50\AA$ $Al_{0.8}Ga_{0.2}As$ spacer.

The acoustical phonons in the proposed layered structure can be evaluated using a matrix method implementation of the standard elastic continuum description of sound waves originally proposed by Rytov. [14] With this model one can obtain the transmission of acoustical waves through the structure, and the displacement pattern as a function of the phonon energy. In Fig.2(top) we display the calculated phonon reflectivity for energies around the first zone-center minigap. For this calculation standard material parameters (sound velocities and densities) were used. [15] A phonon-transmission stop-band is observed, coincident with the SL's minigap. Within this stop-band a phonon-cavity mode exists, characterized by complete transmission of the vibrational energy. The calculated phonon amplitude for this latter mode is shown in Fig.3. While phonon modes with energies within the SL's minigap decay exponentially in space, the phonon-cavity mode propagates through the structure, and its intensity is enhanced within the cavity spacer.

The design of the phonon-cavity deserves some consideration. In principle, any of the acoustical minigaps can be used as phonon DBR. The center of the phonon stop-band (and hence the energy of the confined mode) is simply determined by the SL's period $d = d_1 + d_2$.

The stop-band width, on the other hand, is proportional to a modulation parameter ϵ and displays an oscillatory behavior as a function of the SL layers thickness ratio d_1/d_2. [12] Here $\epsilon = (\eta_2 - \eta_1)/(\eta_1\eta_2)^{1/2}$, with $\eta_i = \rho_i v_i$, ρ_i and v_i the acoustic impedance, density and sound speed of layer i, respectively. The oscillatory function, and thus the thickness ratio d_1/d_2 appropriate for the DBR's of a phonon-cavity, depends also on the order of the minigap ν. For the first zone-edge minigap ($\nu = 1$) the cavity is optimized using $d_1/v_1 = d_2/v_2 = d_c/2v_c$, while for the first zone-center minigap ($\nu = 2$) the relation is $d_1/v_1 = d_2/3v_2 = d_c/2v_c$. Here $d_c(v_c)$ is the cavity thickness (sound velocity). These expressions can be directly transferred to optical waves by replacing the acoustic impedances in ϵ by the refractive indices n_i. In fact, for GaAs and AlAs it turns out that ϵ is basically the same for phonons and photons (0.18 and 0.175, respectively), implying that similar DBR reflectivities and cavity Q-factors can be obtained as a function of the number of DBR layers (N). For our phonon cavity, designed to operate at the first zone-center minigap with 11 SL periods, $Q \sim 140$. On the other hand, Q-factors in the range $Q > 3000$ can be easily obtained with $N \sim 20$.

The issue we address next is how to create and study the confined vibrational excitations in phonon cavities. Superconducting tunnel junctions have been used in the past as sources and detectors of high-frequency phonons with, however, limited resolution. [13] As derives from Fig. 2, we require a technique able to resolve ~ 0.1 cm^{-1} (i.e., 10^{-2} meV) in the energy range $\sim 5-30$ cm^{-1} (1-4 meV). We propose Raman experiments based in a planar microcavity scattering geometry that, besides providing the required resolution [12] and an amplified efficiency ($\sim \times 10^5$), [6,7] give access to the zone-center excitations through the forward-scattering contribution. [7] As we will show next, these singular characteristics allow the observation of these novel acoustical phonon excitations.

We consider a phonon-cavity embedded optical microcavities as depicted in Fig.1. We have performed calculations of the Raman spectra of the proposed structure based on a photoelastic model for the Raman efficiency. Within a photoelastic model for scattering by longitudinal acoustic phonons the Raman efficiency is given by $I(\omega_{q_z}) \propto \left| \int dz E_L E_S^* p(z) \frac{\partial \Phi(z)}{\partial z} \right|^2$, where $E_L(E_S)$ is the laser(scattered) field, $p(z)$ is the spatially varying photoelastic constant, and Φ describes the (normalized) phonon displacement. [12] For an infinite periodic SL the wavevector q_z is a good quantum number. For a standard Raman scattering geometry, with laser and scattered fields given by plane waves ($E_L E_S^* = e^{(k_L - k_S)z}$), $I(\omega_{q_z})$ leads to the usual phonon doublets with transferred wavevector given by the conservation law $q_z = k_L - k_S$. For the case we are discussing, however, q_z is only partially conserved due to the finite-size of the structure. [6,16] In addition, E_L and E_S correspond to the cavity confined photons. Under double optical resonance conditions (that is, both laser and Stokes fields resonant with cavity modes), [6] the incident and scattered photon fields are given within the optical cavity spacer by the same standing wave $E_L = E_S = e^{ik_z z} + e^{-ik_z z}$ (here, by construction, $k_z = \pi/D$ with D the spacer width). [7] Consequently, $E_L E_S^* \propto |E(z)|^2 = 2 + \left(e^{i2k_z z} + e^{-i2k_z z}\right)$. Thus, both a forward scattering (the term 2) and a backscattering contribution $\left(e^{i2k_z z} + e^{-i2k_z z}\right)$ are coherently added to the Raman efficiency $I(\omega_{q_z})$. The former corresponds to a wavevector transfer $q_z = 0$, while for the latter $q_z = 2\pi/D$.

We show in Fig.2, together with the phonon reflectivity curve, a calculated Raman spectrum for the phonon-cavity embedded photon-cavity of Fig.1. For this calculation the laser wavelength is $\lambda = 833$ nm, the layers refractive indices $n_{GaAs} = 3.56$ and $n_{AlAs} = 2.97$ and, being λ in the transparency region, the photoelastic constants are taken real. [12,15] For discussion purposes we also present, in the bottom panel, the separate contributions of the forward scattering (FS) and backscattering (BS) terms. Note that the main Raman peak in Fig.2 corresponds to scattering by the phonon-cavity confined mode. Interestingly, this latter feature comes *only* from the FS ($q_z = 0$) contribution. Its relatively large intensity is explained by the spatial confinement of the cavity-phonon mode at the same place where the confined cavity *photon* has the largest amplitude. In addition, several other features should be noted in the calculated spectra: (i) besides the confined phonon mode, the FS contribution displays scattering at the low energy side of the minigap, corresponding to the (-1) zone-center SL folded minigap mode. [12] The (+1) peak is forbidden in an infinite SL due to a parity selection rule, [12] and is only weakly perceptible in the shown spectra due to a partial relaxation of q_z-conservation due to the phonon-cavity SL mirror's finite-size. (ii) The BS contribution, on the other hand, displays the usual SL phonon doublet. (iii) Side oscillations are observed that modulate the spectra. These oscillations originate in the SL's finite-size, [17,18] and are particularly intense in the cavity spectrum because they add coherently from the BS and FS terms. With "coherence" here we mean that the BS and FS contributions are added *before* (and not after) squaring in $I(\omega_{q_z})$. And last, (iv) the coherent addition of BS and FS in the total cross section is particularly clear around ~ 14 cm^{-1} where the cavity spectrum is not the simple sum of the individual contributions.

With the above Raman calculations in mind we fabricated, using standard molecular beam epitaxy techniques, a phonon-cavity embedded optical cavity with the structure and nominal layer thicknesses as given in Fig.1. The structure was purposely grown with a slight taper which enables a tuning of the optical cavity mode by displacing the laser spot on the sample surface. The layer

widths were chosen so that the optical cavity mode falls below the GaAs gap, in order to avoid parasitic luminescence coming from the substrate. The coupling of both laser and Stokes (non-degenerate) photons with the optical cavity mode is accomplished by tuning the incidence angle as described in Ref. [6]. Since the acoustical folded-phonon-like excitations are in the range 10-30 cm^{-1} (*i.e.*, $\sim 1-4$ meV), incidence angles around $\sim 3-5°$ are required. The Raman experiments were performed at 77 K using a triple Jobin-Yvon T64000 spectrometer equipped with a N_2-cooled charge-coupled-device. A Ti-sapphire laser was used as the excitation source (power below 20 mW) at energies in the range 830-850 nm, well below the SL's fundamental exciton absorption ($\sim$ 1.6 eV=775 nm) and GaAs gap (1.515 eV=820 nm). The spectra were acquired using a triple subtractive configuration with spectral resolution around 0.1-0.2 cm^{-1}.

We show in Fig. 4 a typical experimental spectrum in the spectral range corresponding to the acoustical folded-phonon first zone-center minigap and obtained with laser wavelength $\lambda = 833$ nm. The *optical* cavity mode linewidth, determined mainly by the collection solid angle ($f/2.5$ optics) and the laser spot diameter, was around 10-12 cm^{-1}. This implies that no peak is selectively amplified, and thus that the relative intensity of the different spectral features is intrinsic. [6] To display only the Raman contribution a weak luminescence lorentzian background corresponding to the optical cavity mode was subtracted in the shown spectrum. Identical spectra were acquired from different spot positions and with varying laser energies. A main peak centered at ~ 15 cm^{-1} is observed, together with secondary lines and oscillations. In Fig.4 we also show for comparison the calculated Raman curve corresponding to the nominal structure. The agreement with the experimental curve is remarkable *without any adjustable parameter*. This includes the observation of the sought phonon-cavity mode, but also almost every other detail of the spectra. In fact, the only apparent difference is the predicted (and non observed) splitting of the peak in the low energy side of the phonon minigap (~ 14.3 cm^{-1}). This latter peak corresponds to the (-1) component of the zone-center doublet, mainly determined by the FS contribution (see Fig.2). Its detailed shape is strongly dependent on the interference between the FS and BS terms. As we will show next, the non-observation of the peak splitting can be understood as due to a small but expectable disorder due to interface roughness.

We have considered three possible mechanisms to account for the non-observation of the above discussed FS peak splitting, namely (i) differences of the real structure phonon-cavity spacer width with respect to the nominal value, (ii) destructive interferences in the Raman cross section originated in differences of the widths of the two (otherwise perfect) SL's [17] and, finally (iii) interface roughness leading to width variations around the nominal value for all the layers making the two SL's. We found that only the last choice can explain the observed spectra with reasonable values of disorder. This is shown in Fig.4, with a curve obtained by adding 300 spectra corresponding to phonon-cavities with SL layer widths with random disorder $\pm 4\%$ around the nominal values. This corresponds to changes of $\pm 2.8 \AA$, or ± 1 GaAs or AlAs atomic monolayers at the interfaces. All peaks besides the 14.3 cm^{-1} line are quite stable to this disorder, and thus do not change except for a line broadening which reproduces almost exactly the measured spectral widths. The splitting of the 14.3 cm^{-1} peak, on the other hand, is washed out in correspondence with the experiment. In fact, as it is clear from Fig.4 the agreement between theory and experimental results is striking when the interface roughness is taken into account. This agreement includes the observation of all the main lines and most of the weaker oscillations, their spectral positions and peak widths.

In conclusion, we have proposed a phonon-cavity that displays novel confined acoustical excitations. In addition, we showed through photoelastic model calculations that these vibrations can be generated and probed by Raman scattering experiments that exploit the enhancement and confinement of photons in optical microcavities. Last, we fabricated a phonon-cavity embedded optical microcavity based in GaAs and AlAs materials, and succeeded in observing the cavity-confined high frequency hyper-sound mode. Calculations that take into account a small but expectable interface roughness are able to account precisely for every detail of the observed spectra. The confined phonon modes in a phonon cavity are spatially localized highly mono-energetic excitations. These features open the way to studies of phonon stimulation, coherent phonon generation, and modified (enhanced or inhibited) electron-phonon interactions in phonon cavities. The confinement and enhancement of photons in an optical microcavity can be exploited, in addition, for the optical generation of these confined phonon modes.

[1] C. Kittel, in *Introduction to solid state physics* (New York, Wiley, 1986).
[2] P. Yeh et al., J. Opt. Soc. Am. **67**, 423 (1977).
[3] E. Yablonovitch, Phys. Rev. Lett. **58**, 2059 (1987); E. Yablonovitch and T. J. Gmitter, *ibid* **63**, 1950 (1989).
[4] *Confined Electrons and Photons: New Physics and Applications*, edited by E. Burstein and C. Weisbuch (Plenum, New York, 1995).
[5] R. P. Stanley et al., Phys. Rev. A **48**, 2246 (1993).
[6] A. Fainstein et al., Phys. Rev. Lett. **75**, 3764 (1995).
[7] A. Fainstein et al., Phys. Rev. Lett. **86**, 3411 (2001).
[8] E. B. Tucker, Phys. Rev. Lett. **6**, 547 (1961).
[9] H. Haken, *Quantum Field Theory of Solids. An Introduction*, (North Holland, Amsterdam, 1976), p. 218.
[10] P. A. Fokker et al., Phys. Rev. B **55**, 2925 (1997).
[11] See, e.g., T. Dekorsy, G. C. Cho, and H. Kurz, in *Light Scattering in Solids VIII*, edited by M. Cardona and G. Güntherodt (Springer, Heidelberg, 2000), p. 169.
[12] B. Jusserand and M. Cardona, in *Light Scattering in Solids V*, edited by M. Cardona and G. Güntherodt (Springer, Heidelberg, 1989), p. 49.
[13] V. Narayanamurti et al., Phys. Rev. Lett. **43**, 2012 (1979).
[14] S. M. Rytov, Akust. Zh. **2**, 71 (1956).
[15] S. Adachi, J. Appl. Phys. **58**, R4 (1985).
[16] M. Trigo et al.,(unpublished).
[17] M. Giehler et al., Phys. Rev. B **55**, 7124 (1997).
[18] P. X. Zhang et al., Can. J. Phys. **70**, 843 (1992).

FIG. 1. Scheme of the proposed phonon-cavity embedded optical cavity. The phonon "mirrors" consist of 11 period $74\AA/38\AA$ GaAs/AlAs SL's, and enclose a $50\AA$ $Al_{0.8}Ga_{0.2}As$ spacer. The phonon-cavity structure, on the other hand, constitutes the λ spacer of an optical microcavity enclosed by 20 DBR $Ga_{0.8}Al_{0.2}As$/AlAs pairs on the bottom and 16 on top.

FIG. 2. Calculated phonon reflectivity (top) and Raman spectrum (bottom) in the spectral region around the first zone-center minigap for the phonon-cavity embedded photon-cavity depicted in Fig.1. The separate contributions of the forward scattering (FS) and backscattering (BS) terms is also shown.

FIG. 3. Calculated phonon amplitude corresponding to the confined phonon-cavity mode. The curve is shown superimposed to a scheme of the phonon structure characterized by the materials photoelastic constant.

FIG. 4. Experimental Raman spectrum in the spectral range corresponding to the acoustical folded-phonon first center-zone minigap (Exp.), obtained with laser wavelength $\lambda = 833$ nm. Also shown are calculated Raman curves corresponding (*i*) the nominal structure (Nominal), and (*ii*) a phonon-cavity with random disorder $\pm 4\%$ of the SL layer's thickness (Disorder).

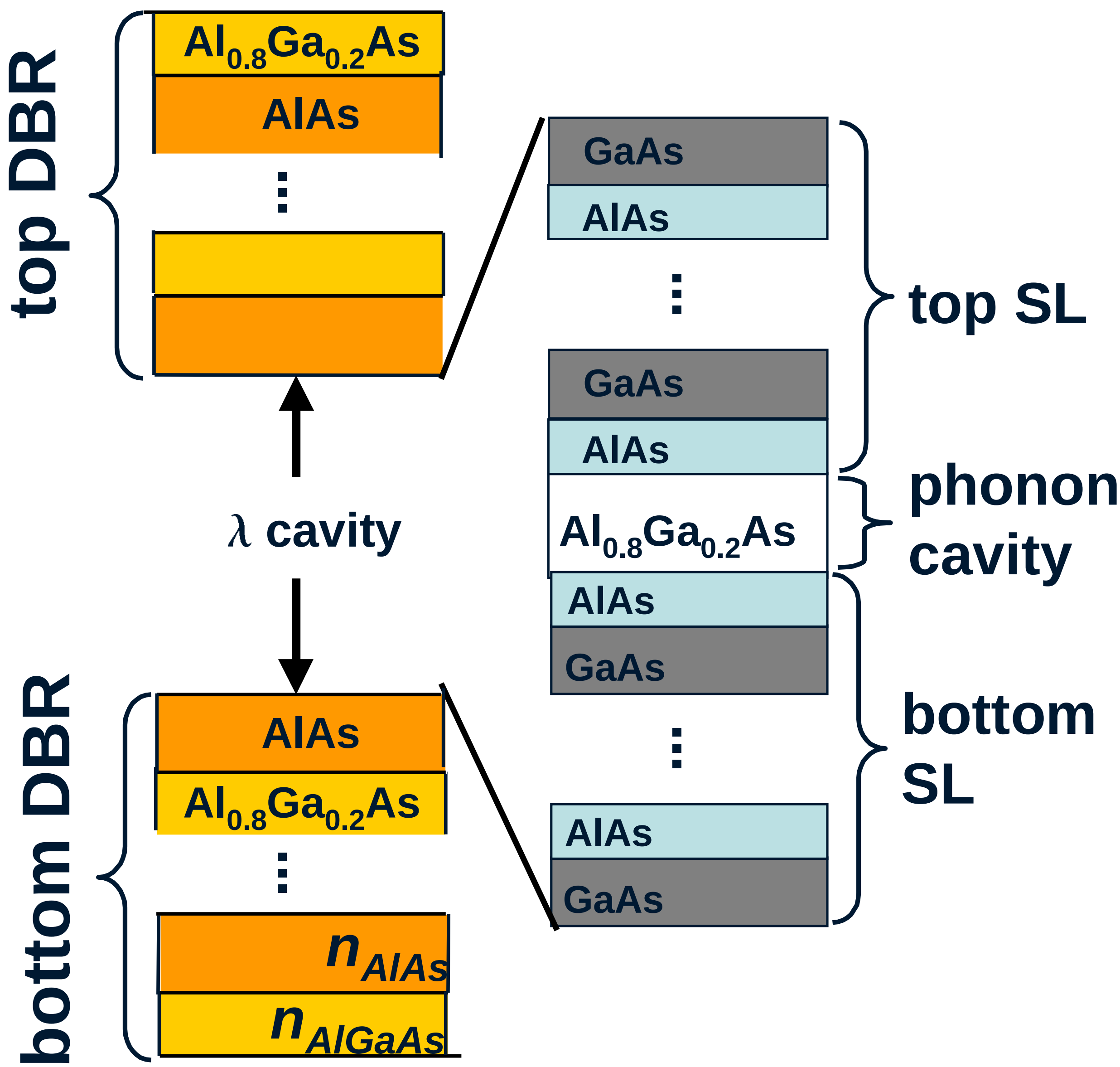
top DBR
$Al_{0.8}Ga_{0.2}As$
AlAs
GaAs
AlAs
top SL
GaAs
AlAs
phonon cavity
$Al_{0.8}Ga_{0.2}As$
λ cavity
AlAs
GaAs
bottom SL
AlAs
GaAs
bottom DBR
AlAs
$Al_{0.8}Ga_{0.2}As$
n_{AlAs}
n_{AlGaAs}

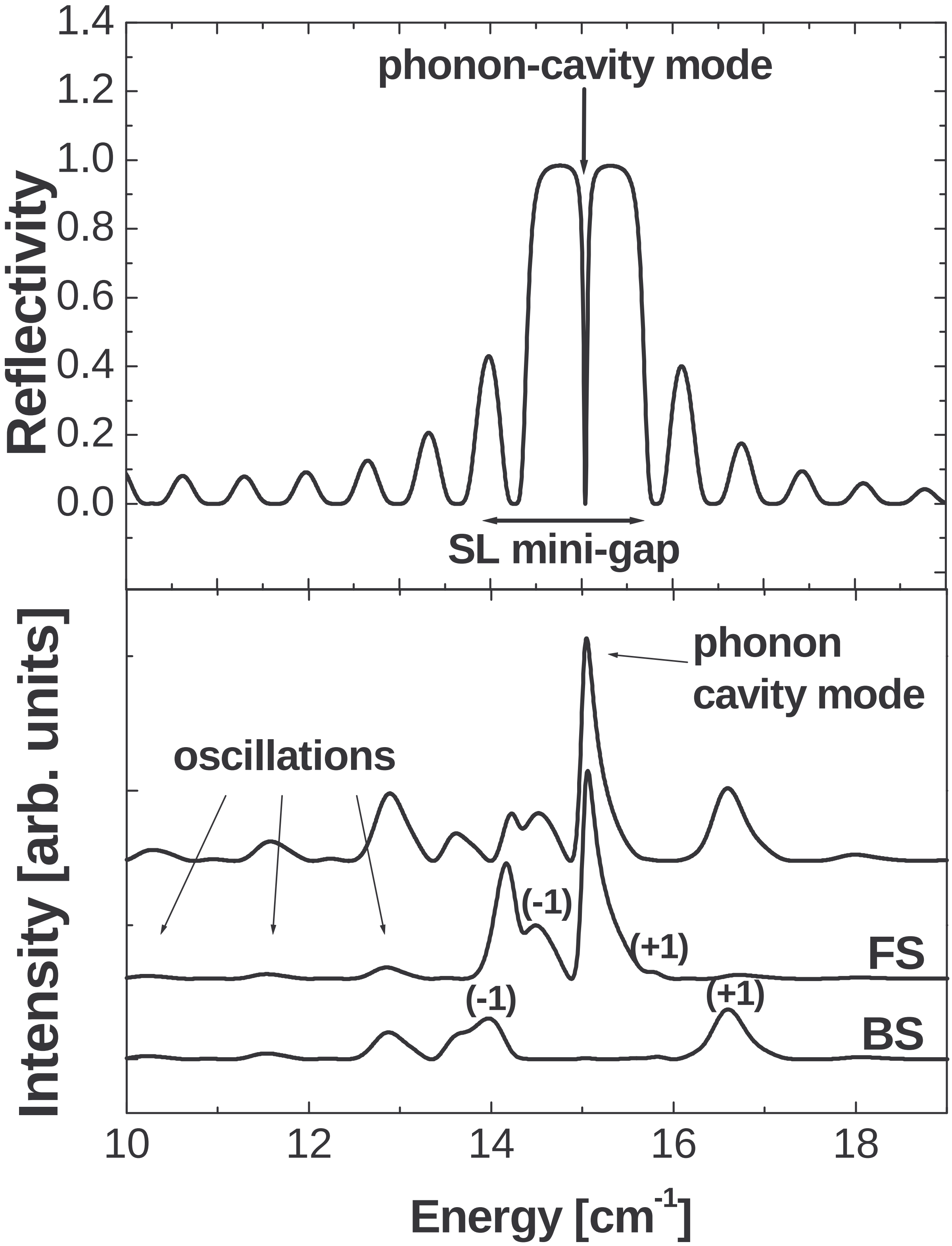

phonon-cavity mode
SL mini-gap
Reflectivity
1.4
1.2
1.0
0.8
0.6
0.4
0.2
0.0
phonon
cavity mode
oscillations
(-1)
(+1)
FS
(-1)
(+1)
BS
Intensity [arb. units]
10
12
14
16
18
Energy [cm-1]

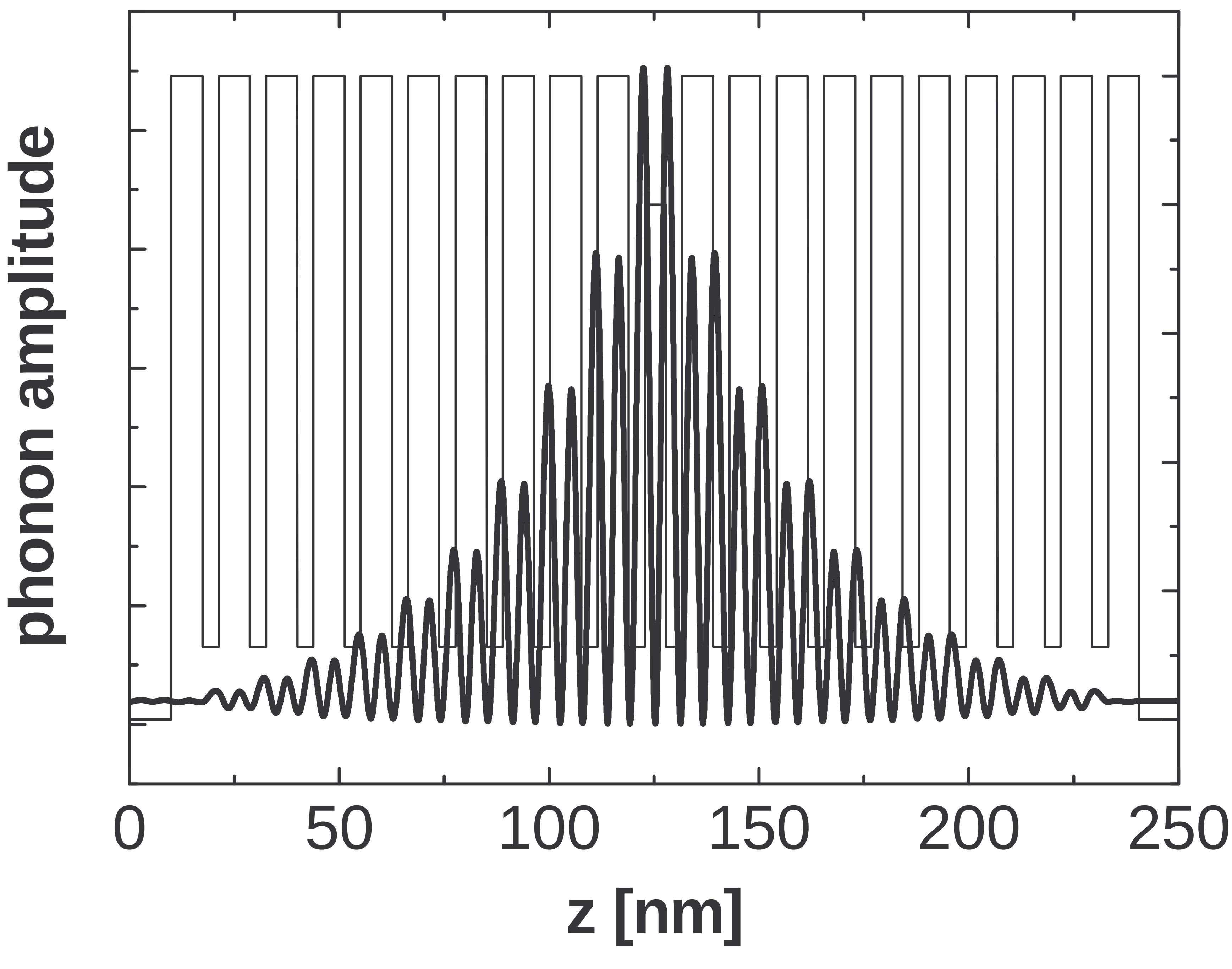

phonon amplitude
0
50
100
150
200
250
z [nm]

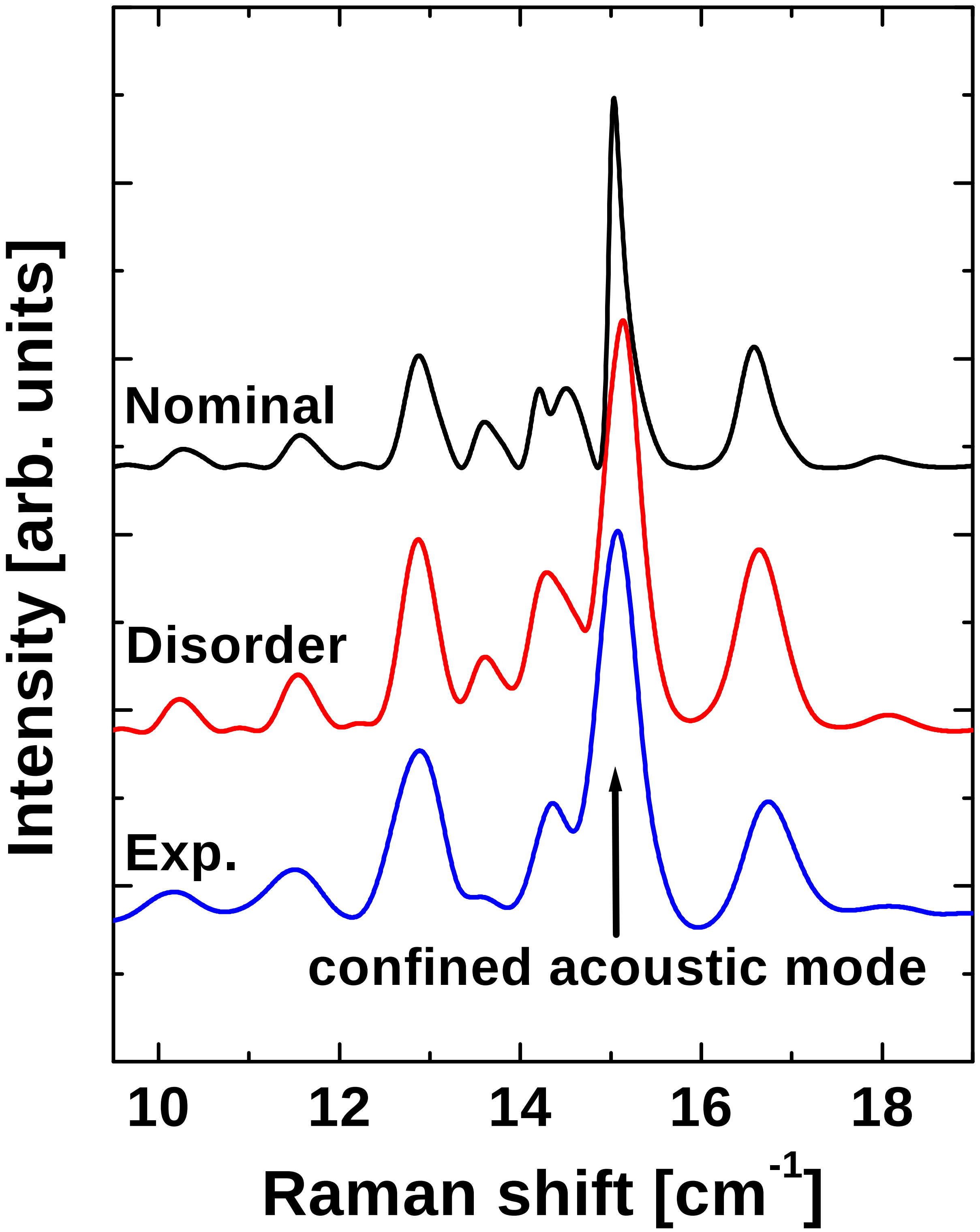
Nominal
Disorder
Exp.
confined acoustic mode
Intensity [arb. units]
10
12
14
16
18
Raman shift [cm^{-1}]